Preprint
UCRL-JC-147936

# Advances Toward Inner-Shell Photo-Ionization X-Ray Lasing at 45 Å

*S.J. Moon, F.A. Weber, P.M. Celliers, D.C. Eder*

This article was submitted to 8th International Conference on X-Ray Lasers, Aspen, CO, May 27-31, 2002

**July 18, 2002**

*U.S. Department of Energy*

Lawrence
Livermore
National
Laboratory

DISCLAIMER



This work was performed under the auspices of the United States Department of Energy by the University of California, Lawrence Livermore National Laboratory under contract No. W-7405-Eng-48.

# Advances toward inner-shell photo-ionization x-ray lasing at 45 Å

Stephen J. Moon, Franz A. Weber, Peter M. Celliers, and David C. Eder

*Lawrence Livermore National Laboratory, Livermore, CA 94551*

**Abstract.** The inner-shell photo-ionization (ISPI) scheme requires photon energies at least high enough to photo-ionize the K-shell, ~286 eV, in the case of carbon. As a consequence of the higher cross-section, the inner-shell are "selectively" knocked out, leaving a hole state $1s2s^22p^2$ in the singly charged carbon ion. This generates a population inversion to the radiatively connected state $1s^22s^22p$ in C+, leading to gain on the 1s-2p transition at 45 Å. The resonant character of the lasing transition in the single ionization state intrinsically allows much higher quantum efficiency compared to other schemes. Competing processes that deplete the population inversion include auto-ionization, Auger decay, and in particular collisional ionization of the outer-shell electrons by electrons generated during photo-ionization. These competing processes rapidly quench the gain. Consequently, the pump method must be capable of populating the inversion at a rate faster than the competing processes. This can be achieved by an ultra-fast, high intensity laser that is able to generate an ultra-fast, bright x-ray source. With current advances in the development of high-power, ultra-short pulse lasers it is possible to realize fast x-ray sources based that can deliver powerful pulses of light in the multiple hundred terawatt regime and beyond. We will discuss in greater detail concept, target design and a series of x-ray spectroscopy investigations we have conducted in order to optimize the absorber/x-ray converter – filter package.

## 1. INTRODUCTION

Since the first demonstration of x-ray lasing at Lawrence Livermore National Laboratory in 1985 [1], and elsewhere [2], based on the utilization of high-power pump lasers designed and built for fusion research, new and more efficient pumping techniques have been vigorously sought after. In the last decade, many important experiments have been conducted and good progress has been made towards table-top x-ray lasers. The advent of a new generation of chirped pulse amplification techniques has made possible the design and fabrication of powerful and ultra-short pulse duration pump lasers that seem to have the capability to shrink source dimensions from occupying whole rooms to table-top size. Many applications, however, do indeed require x-ray laser wavelengths shorter than currently attainable with table-top sized schemes since scaling to wavelengths shorter than 100 Å proves rather difficult [3] – [7].

Inner-shell photo-ionization x-ray lasers represent a class of x-ray lasers previously unrealized and first proposed by Duguay and Rentzepis [8]. Several authors have since

adopted that inner-shell photo-ionization scheme [9, 10], and conclude that operating on a Kα transition of a low Z element constitutes an attractive way to efficiently pump an x-ray laser in the sub 50 Å regime. All these new schemes still need sub 50 femtosecond and greater than 1 J in an optical pulse to drive the transition. Advances in powerful ultrashort pulse laser (USPL) technology prompted us to investigate that group of schemes with the application of carbon as the lasant material in greater detail. The choice of this material is by virtue of its electronic properties with particular respect to the Auger recombination rate and lasing wavelength at a wavelength of 45 Å.

Here, in section 2 we discuss physics of the target and present our modeling results. We describe our method for a traveling wave setup suitable to pump inner-shell photo-ionization schemes in section 3. The report on our experimental findings on target output and laser performance is given in section 4. We summarize in section 5.

## 2. Target Physics

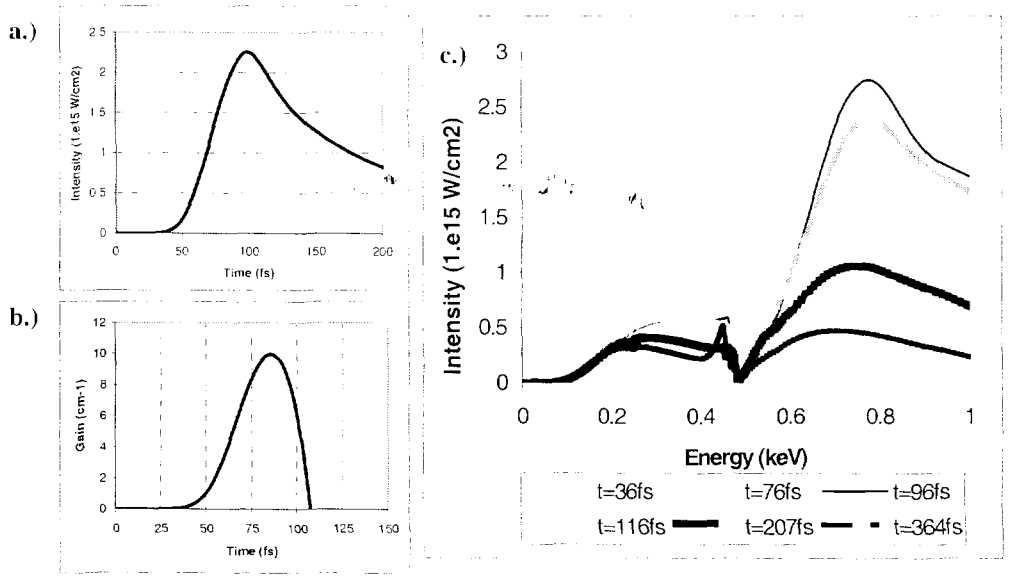


Figure 1. (a.) Shows the simulated temporal history of the source, spectrally integrated. (b.) Is the calculated gain in carbon lasant ($10^{18}$ $cm^{-3}$ foam) at 45 Å. (c.) Shows the simulated spectral emission for various times.

Results of our modeling effort are shown in figures 1 a through c. An USP high intensity optical laser of $1x10^{17}$ $W/cm^2$ and 40 fs pulse duration is incident on a foil consisting of 200 Å layered on 1000 Å of Ti. The laser is at normal incidence on the gold absorber, the front side of the target, and the incoherent x-ray source, which pumps the carbon lasant, is due to back-side emission. The modeling was performed using the hydrodynamics/atomic code LASNEX [11]. The code includes many physics models necessary to simulate a multidimensional radiative hydrodynamics problem, including laser-matter interaction, radiation transfer, electron thermal diffusion by

conduction, and simple description of non-local thermodynamic equilibrium atomic kinetics. Reference 11 includes a description of the physics models used in LASNEX.

The energy from the optical laser is deposited in a self-consistent manner by solving the wave equation for the laser electro-magnetic field and the atomic kinetics and x-ray emission are calculated with an average-atom atomic model, which includes spin orbit coupling. Careful optimization of the converter/filter assembly parameters yielded the values indicated above. Furthermore, the ionization velocity in the absorber material ensures that the thin gold layer is completely ionized at the end of a ~ 40 fs optical pump pulse, and at the same time the absorption occurs at near solid density. Figure 4 a shows the calculated backside emission from the foil structure and figure 1 b shows the corresponding gain of 9.9 $cm^{-1}$ for low-density carbon foam at $10^{18}$ $cm^{-3}$. Figure 1 c depicts spectral emission from the target structure for various times.

## 3. Traveling Wave Pumping of an Ultrashort Pulse X-Ray Laser

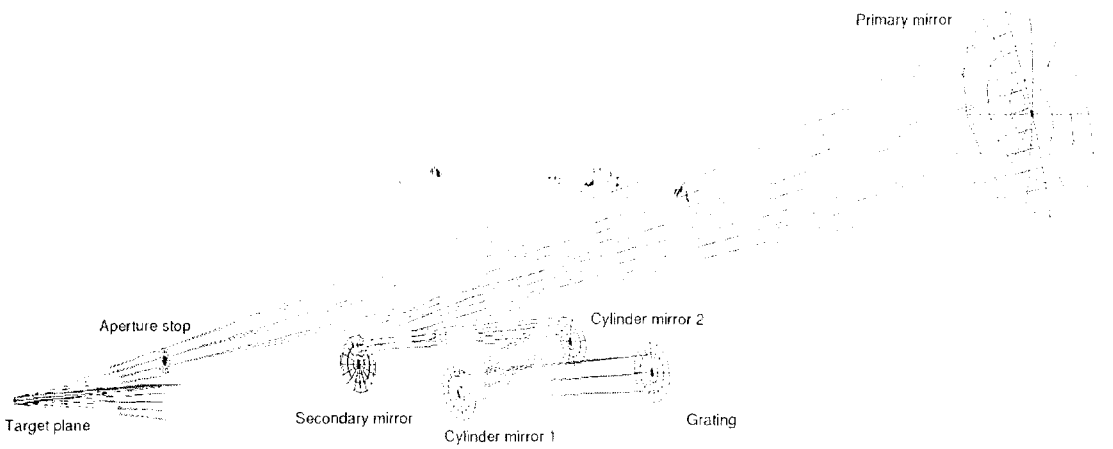


Figure 2. USPL traveling wave pumping system in line focus geometry.

The use of traveling optical waves as a method of delivering optical energy is not new to laser science [12] – [16]. Even before chirped pulse amplification (CPA) came on the scene, Bor [17] employed a traveling wave technique to produce optical pulses with a 1 picosecond duration. Indeed, the field of collisionally pumped XRLs has also seen the implementation of traveling wave pumping (TWP) schemes, although at much longer pulse durations, in order to enhance XRL performance. Previous analysis [18] for these schemes shows that TWP may be advantageously applied whenever the pump time divided by the target length turns out to be less than 33 ps/cm.

The physical characteristics of the required traveling wave optical pumping system are largely determined by the physics of the x-ray laser transition as described in section 2. The very rapid rise time of the broad-bandwidth x-ray source, faster than the upper state lifetime in carbon, dictates, because of the competing processes and subsequent depopulation of the lower laser state, zero gain for times greater than

approximately 80 fs (see figure 1 b). This time constraint is true for every incremental length of the lasing volume. Thus, we find that the stringent pump requirements of the ISPI XRL scheme as a consequence also impose very stringent requirements on the quality and fidelity of the focusing system. A traveling wave focusing scheme is therefore essential to pump an XRL amplifier target.

The pump light (optical energy of USPL) must be delivered to the target at an intensity of 1.0 x $10^{17}$ W/cm$^2$ in a spot size of approximately 30 μm that illuminates the target along a linear track of ~ 10 mm length and traveling at the velocity of light c (index of refraction ~ 1.000) along the target surface. The arrival time deviation from a linear variation at any point along the trajectory must be less than 50 fs corresponding to a distortion level around $10^{-4}$ or better. The pulse duration of the focused beam must be a faithful representation of the incident pulse from the drive laser. Also attendant is the vertical spatial distortion that, accordingly, must be limited to better than +/- 15 μm over 10 mm or ~ $10^{-3}$ over the laser length. These are not unreasonable numbers for generic optical systems; however, the utilization of a high power USPL with its 50 to 100 nm bandwidth mandates all-reflective optical surfaces in order to eliminate not only the chromatic distortions that lead to pulse temporal broadening [19], but also distortions due to the intensity induced nonlinear index of refraction variations (B-Integral). As a result, only a vacuum diffraction grating succeeds as a dispersive element out of a variety of traditional methods (prisms, Fabry-Perot interferometers, and gratings [20], [21]) to tilt wave fronts of optical pulses by angular dispersion.

The schematic of the TWP setup is depicted in figure 2. The novel feature of the design is a holographically-generated grating that serves both, to produce the pulse front tilt needed for the traveling wave, and also to correct residual aberrations in the focusing system. We designed the system to project an image of an incident 50 mm beam onto the 10 mm target surface at 5x demagnification. Most of the focusing power is accomplished using a reflective inverted off-axis Schwarzschild microscope configuration (primary mirror: 1500 mm concave radius, secondary mirror: 309 mm convex radius). These two mirrors are placed in a classic Schwarzschild confocal configuration – and the design is optimized for 5:1 demagnification. The grating is centered on, and perpendicular to, the chief axis of the Schwarzschild system; the grating image is then projected onto the target plane, which is also centered on and perpendicular to the chief axis. In our design we use an off-axis subset of the cylindrically symmetric Schwarzschild configuration, hence the rays traveling through our focusing system arrive obliquely on all the optics. In order to produce a pulse front traveling at velocity c across the target surface using an imaging system operating with magnification M, it can be shown that the grating must be illuminated at an angle q = $\sin^{-1}$(M) from the grating normal (while the diffracted beam leaves the grating approximately at the normal). In our case M = 0.2 and q = 11.54°. The pulse front intersects the grating surface along a vertical line; this line must be focused onto the target at a point, which requires the focusing system to be astigmatic. We accomplish this by using two additional cylindrical mirrors that are configured to produce the required line focus on the target. Using the combination of the two spherical and two cylindrical elements a ray trace analysis can optimize this system to

produce a line focus that is a few times diffraction-limited at the target plane. The trajectory of the pulse front produced by imaging a flat grating onto a flat target will not have a constant velocity, but will have a small quadratic deviation from this. (A planar pulse front originating from the grating reaches the target plane as a cylindrical pulse front because it must pass through a focus before reaching the target.) We can adjust the shape of the pulse front to correct for this by using a slightly cylindrical surface at the grating plane. The required grating surface curvature depends on the magnification and focal length of the Schwarzschild system.

The remaining geometrical aberrations in the system can be corrected by generating the grating holographically. To accomplish this the system must be back-illuminate with a diffraction limited line focus at the target plane. The grating can then be produced by interfering the back propagating beam with the 11.54° incident beam at the grating surface. The back propagating beam incorporates the residual aberrations in the focusing system, thus allowing the production of a grating pattern that will correct for these aberrations. During operation slight adjustments in the phase velocity of the pump at the target can be accomplished by slight tilts of the grating about an axis perpendicular to the plane of incidence.

## 4. Experimental Results

In order to effectively and accurately investigate the emission from the x-ray converter it is necessary to field a spectrometer, which covers wavelength regions on both the long and short wavelength side of the carbon K-edge. That requirement puts severe limitations on the choice of materials to be employed in the dispersing element of the detection system.

The experimental investigation was conducted at the LLNL Falcon USPL facility. The laser is based on a Ti:Sapphire oscillator and uses CPA to produce nominally 500 mJ pulses of 35 fs individual duration at a repetition rate of 1 Hz. We used the laser's regenerative amplifier pumped at saturation level. After initial determination of output levels all shots were set up in a p-polarized configuration and a 45 degree angle of incidence on target was maintained. The center wavelength of the laser l = 820 nm was focused on target by means of an off-axis parabola at f/2. In our first set of experiments we have used maximum energy through the four pass amplifier and air compressor and have been able to achieve around 100 mJ on target. On every shot we monitored the unconverted beam energy as well as the level of amplified spontaneous emission (ASE) by means of a calorimeter and a 170 ps fast-rise time photodiode, respectively. A typical ASE profile rose linearly in time until the arrival of the main pulse.

The CCD as well as a soft x-ray pinhole camera (SXR PHC) were filtered in order to block stray light and unwanted optical reflections. We used 12.5 μm of beryllium for the SRX PHC whereas we installed a total of 2kÅ of aluminum on top of 2 kÅ of Lexan in the spectrometer. The spectral composition of backside x-ray emission for various focal distances is shown in figure 3. For verification of the focal spot size on

the target front side we employed an x-ray pinhole camera comprising a multiple pinhole array coupled to a soft x-ray sensitive CCD as described above. The diagnostic was operated at a magnification of 15. Data analysis on both, the pinhole images and the static spectroscopy data was performed by subtracting dark images in order to correct for detector temperatur-dependent noise in addition to the subtraction of high energy photon and electron generated background. We then integrated the signal over the regions of interest and adjusted for analyzer reflectivity, filter transmission functions, and detector quantum efficiency.

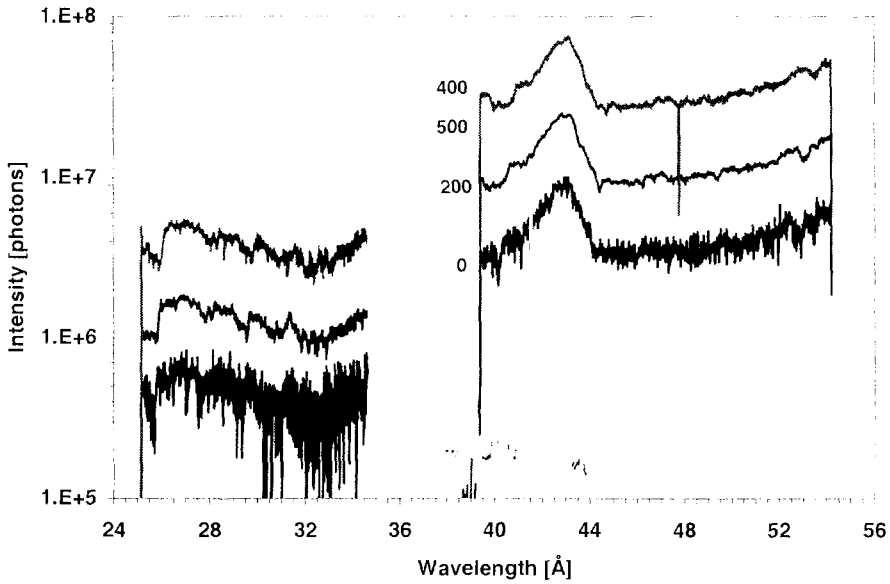


Figure 3: Time integrated backside emission increases away from best focus.

We found the spot size at best focus to be around 23 μm at FWHM, which corresponds to a laser intensity on target of $6.9 \times 10^{17}$ W/cm$^2$. The best focus is located at a position measuring 100 μm away from the initial target surface due to a distance calibration offset.

## 5. CONCLUSIONS

We have set out to pursue a longstanding goal of x-ray laser research, the realization of the inner-shell photo-ionization (ISPI) pumping scheme in order to demonstrate lasing at wavelengths not yet possible by table-top energy sources. We have shown an efficient x-ray converter/filter package and studying its backside x-ray emission. For that purpose we have devised and fabricated a versatile soft x-ray spectrometer universally suitable for analysis of various x-ray sources based on laser produced plasmas. A soft x-ray pinhole camera has been used as an additional diagnostic to verify focal spot properties and target intensities. We found a maximum conversion efficiency of $1.2 \times 10^{-4}$ at a position of 300 μm out of best focus. We did not see any

evidence for increased backside x-ray emission as a result of intentional prepulses delivered to the target, independent of pulse delay.

We have also invented a novel technique to measure the rise time of ultrafast x-ray pulses, which constitutes an enabling technology in the diagnosis of modern 4th generation light sources currently under design worldwide. There, we employ a diamond x-ray transducer in a pump probe arrangement to reflect a p-polarized probe beam at Brewster's angle. In addition, we have shown how to create a line focus using an ultrashort optical laser pulse in traveling wave geometry employing a holographically produced grating for compensation of optical aberrations in the relay imaging system, which are introduced by the use of standard spherical and cylindrical components.

## ACKNOWLEDGEMENTS

This work was performed under the auspices of the U.S. Dept. of Energy by the University of California Lawrence Livermore National Laboratory, through the Institute for Laser Science and Applications, under Contract No. W-7405-Eng-48.

## REFERENCES

1. D. L. Matthews et al., Phys. Rev. Lett. **54**, 110 (1985).
2. S. Suckewer et al., Phys. Rev. Lett. **55**, 1753 (1985).
3. J.J. Rocca et al., Phys. Rev. Lett. **77**, 1476 (1996).
4. B.E. Lemoff et al., Phys. Rev. Lett. **74**, 1574 (1995).
5. Y. Nagata et al., Phys. Rev. Lett. **71**, 3774 (1993).
6. P. V. Nickles et al., Phys. Rev. Lett. **78**, 2748 (1997).
7. J. Dunn et al., Phys. Rev. Lett., **80**, 2825 (1998).
8. M. A. Duguay and P. M. Retzepis, Appl. Phys. Lett. **10**, 350 (1967)
9. H. C. Kapteyn, Appl. Opt. **31**, 4931 (1992).
10. S. J. Moon and D. C. Eder, Physical Review A **57**(2), Feb. 1998.
11. G.B Zimmerman and W.L. Kruer, Comments Plasma Phys. Controlled Fusion **2**, 51-61 (1975).
12. M. E. Mack et al., Appl. Phys. Lett. **15**, 166 (1969).
13. R. Wyatt and E. E. Marinero, Appl. Phys. **25**, 297 (1981).
14. H. J. Polland et al., Appl. Phys. B **32**, 53 (1983).
15. M. H. Sher et al., Opt. Lett. **12**, 891 (1987).
16. C. P. J. Barty et al., Phys. Rev. Lett., **61**, 2201 (1988).
17. Zs. Bor, S. Szatmari, and A. Muller, Appl. Phys. B **32**, 101 (1983).
18. J. C. Moreno, J. Nilsen, and L. B. Da Silva, AIP Conf. Proc. **332**, 21 (1994).
19. Z. L. Horvath et al., Opt. Eng. **32**, 2491 (1993).
20. J. R. Crespo Lopez-Urrutia et al.: Proc. SPIE **2012**, 258 (1993).
21. Z. S. Bor et al., Opt. Eng. **32**, 2501 (1993).